

# Shape Complexity in Cluster Analysis

Eduardo J. Aguilar

Instituto de Ciência e Tecnologia

Universidade Federal de Alfenas

Rod. José Aurélio Vilela, 11999

37715-400 Poços de Caldas - MG, Brazil

Valmir C. Barbosa\*

Programa de Engenharia de Sistemas e Computação, COPPE

Universidade Federal do Rio de Janeiro

Centro de Tecnologia, Sala H-319

21941-914 Rio de Janeiro - RJ, Brazil

## Abstract

In cluster analysis, a common first step is to scale the data aiming to better partition them into clusters. Even though many different techniques have throughout many years been introduced to this end, it is probably fair to say that the workhorse in this preprocessing phase has been to divide the data by the standard deviation along each dimension. Like division by the standard deviation, the great majority of scaling techniques can be said to have roots in some sort of statistical take on the data. Here we explore the use of multidimensional shapes of data, aiming to obtain scaling factors for use prior to clustering by some method, like k-means, that makes explicit use of distances between samples. We borrow from the field of cosmology and related areas the recently introduced notion of shape complexity, which in the variant we use is a relatively simple, data-dependent nonlinear function that we show can be used to help with the determination of appropriate scaling factors. Focusing on what might be called “midrange” distances, we formulate a constrained nonlinear programming problem and use it to produce candidate scaling-factor sets that can be sifted on the basis of further considerations of the data, say via expert knowledge. We give results on some iconic data sets, highlighting the strengths and potential weaknesses of the new approach. These results are generally positive across all the data sets used.

**Keywords:** Cluster analysis, Data scaling, Distance-based clustering, Shape complexity.

---

\*Corresponding author (valmir@cos.ufrj.br).

# 1 Introduction

The common wisdom regarding the processing of data prior to cluster analysis, particularly when a distance-based clustering method like k-means or some forms of hierarchical clustering are used, is that data should be scaled to improve results. Even though researchers have been prolific in creating domain-specific forms of scaling (cf., e.g., [1]), already the earliest studies systematically approaching the subject viewed division by the standard deviation or by the range in each dimension as the natural candidates they still are to this day [2,3]. This is not to say that alternative divisors were not considered: they were [4], but the situation seems to have remained largely unchanged until very recently, with the introduction of the so-called pooled standard deviation [5], which continues to support division by the standard deviation unless this would make the dimension in question lose information crucial to partitioning the data into clusters. Should this be the case, a weighted averaged of the standard deviations localized around statistically significant modes in that dimension is used instead. This average is the pooled standard deviation of the data in that dimension, henceforth denoted by  $\sigma_k^{\text{pool}}$  for dimension  $k$ . Notably, the essential motivation for the creation of  $\sigma_k^{\text{pool}}$  seems well aligned with concerns that have been voiced since the late 1960's (cf. [3] for comments on this).

In a similar vein, it has for several decades been clear that some form of optimization problem must exist whose solution yields scale factors that make some sort of sense for the various dimensions. And indeed this has been pursued, though to the best of our knowledge not for the last three decades, at least. Noteworthy representatives of these attempts include optimizing for a linear transformation of the data [6]; maximizing the square of a correlation between two sets of distances between samples [7]; a least-squares method for determining scale factors that make such distances approach those in the dendrogram resulting from hierarchical clustering [8]; and determining scaling factors by considering the modal structure of the data in each dimension in a way that, to a certain degree, prefigures the above definition of the pooled standard deviation [9]. Each of these approaches seems to have either disappointed its own creator [6], or remained tailored to the generally uninteresting cases of nonoverlapping clusters [7], or been tested only superficially [8], or simply remained untested [9].

Here we introduce the use of a shape-complexity function to guide the determination of scale factors. By this denomination we are not referring to one of the many forms of complexity used to characterize the computer representations of three-dimensional shapes [10]. Instead, we refer to a generalization to multiple dimensions of the homonymous three-dimensional concept introduced recently in cosmology and related disciplines [11,12]. If we imagine (up to three dimensions) that the disposition of data samples in space gives the data set an inherent shape, then clearly being able to shrink or stretch each dimension independently of all others is an important source of shape variation, one that we explore for the purpose of cluster analysis. One particular facet of shape complexity that we find especially relevant to this end is that it allows what should

be intercluster distances to be considered side-by-side with distances that should be intracluster. While normally cluster analysts know which distance is which type only in a very limited manner, shape complexity provides a handle that can help in posing a nonlinear programming problem for the automatic determination of scale factors (or rather, candidate scale factors to undergo further scrutiny based on what analysts do know of the domain in question).

We proceed in the following manner. In Section 2 we introduce the form of shape complexity we use, giving its definition and properties of interest. We also discuss why it relates closely to the role of scale factors in cluster analysis and how determining such factors from it can be formulated. We then proceed with a description of our experimental setup, in Section 3. This includes the data sets on which we experiment, the tools and algorithms we use, and how we evaluate a data set's partition into clusters. Importantly, we perform clustering solely via the k-means method, owing mainly to its great potential to perform well when clusters overlap [13], and also to its long history, during which many implementations and variants have appeared [14]. Results and discussion are given in Sections 4 and 5, respectively. We close in Section 6.

## 2 Shape complexity

We consider an  $n_{\text{orig}} \times d$  data matrix  $X$  with  $n_{\text{orig}}, d > 1$ , where  $n_{\text{orig}}$  is the number of  $d$ -dimensional real samples. For  $1 \leq k \leq d$ , we use  $\sigma_k^2$  to denote the samples' variance on dimension  $k$ , and  $\alpha_k > 0$  to denote the scale factor to be used on the samples along this dimension in order to facilitate clustering. Factor  $\alpha_k$  is assumed to be applied to the various  $X_{ik}$ 's along with their division by  $\sigma_k$ . That is, each original  $X_{ik}$  is to undergo scaling by the factor  $\alpha_k/\sigma_k$ . This makes it easier to assess the effect of factor  $\alpha_k$  relative to the more common  $1/\sigma_k$  and also enables some key developments later in this section.

For reasons to be discussed shortly, here we propose that the appropriate  $\alpha_k$ 's be determined with the guidance of the so-called shape complexity of the  $n_{\text{orig}}$  points in  $d$ -dimensional real space that define the samples. This notion is borrowed from the physics of multiple bodies interacting gravitationally with one another. For  $d = 3$  and the points having masses associated with them, shape complexity has been shown to help account for structure as it arises in the form of clusters during the system's evolution [11, 12].

The version of shape complexity we use, denoted by SC, is given by

$$\text{SC} = \left( \sum_{i < j} r_{ij}^2 \right)^{1/2} \sum_{i < j} r_{ij}^{-1}, \quad (1)$$

where each  $i$  and  $j$  are distinct samples and  $r_{ij}$  is the Euclidean distance between them. That is, the number of samples SC takes into account is  $n$  such that  $1 < n \leq n_{\text{orig}}$  (duplicates may thus exist only if  $n_{\text{orig}} > 2$ ) and

$$r_{ij}^2 = \sum_k \alpha_k^2 \rho_{ijk}^2, \quad (2)$$

with

$$\rho_{ijk} = \frac{X_{ik} - X_{jk}}{\sigma_k}. \quad (3)$$

SC is therefore a function of the  $\alpha_k$ 's, but we refrain from denoting this explicitly for the sake of notational clarity. Importantly, the use of  $i < j$  in the summations of Eq. (1) indicates that they occur on the set of all  $\binom{n}{2}$  unordered pairs of distinct samples. Likewise, the summation on  $k$  in Eq. (2) indicates that it occurs over all  $d$  dimensions.

**Radial invariance.** One of the key properties for which SC is appreciated in its fields of origin is scale invariance, which in our terms is to be understood as follows. If  $\alpha_k$  has the same value for every  $k$ , then clearly SC remains unchanged however this common value is varied. But if SC is to be used to improve the results of clustering algorithms on the data, setting every  $\alpha_k$  to the same value is in general not an option. Scale invariance, nevertheless, is a special case of the much more useful radial invariance we discuss next. The radial invariance of SC can be seen in more than one way, but here we choose the perspective of certain directional derivatives of SC. This requires us to already consider the gradient of SC, which will be instrumental later on.

For  $f$  a differentiable function of the  $\alpha_k$ 's, we let  $f'_k$  denote  $\partial f / \partial \alpha_k$ , the  $k$ th component of the gradient of  $f$ , and moreover write  $g = (\sum_{i < j} r_{ij}^2)^{1/2}$  and  $h = \sum_{i < j} r_{ij}^{-1}$  so that  $SC = gh$ . We get

$$SC'_k = g'_k h + g h'_k, \quad (4)$$

where

$$g'_k = \alpha_k g^{-1} \sum_{i < j} \rho_{ijk}^2 \quad (5)$$

and

$$h'_k = -\alpha_k \sum_{i < j} r_{ij}^{-3} \rho_{ijk}^2. \quad (6)$$

Radial invariance comes from realizing that the directional derivative of SC is zero along any straight line extending out from the origin into the positive  $d$ -dimensional real orthant, that is,

$$\sum_k \alpha_k SC'_k = 0 \quad (7)$$

for any valuation of the  $\alpha_k$ 's. To put it differently, SC has the same value at any two assignments of values to  $\alpha_1, \dots, \alpha_d$ , say  $v_1^{(1)}, \dots, v_d^{(1)}$  and  $v_1^{(2)}, \dots, v_d^{(2)}$ , such that  $v_k^{(2)} = t v_k^{(1)}$  for every  $k$  and some  $t > 0$ .

To see how Eq. (7) comes about, simply write

$$g \sum_k \alpha_k \text{SC}'_k = h \sum_k \alpha_k^2 \sum_{i < j} \rho_{ijk}^2 - g^2 \sum_k \alpha_k^2 \sum_{i < j} r_{ij}^{-3} \rho_{ijk}^2 \quad (8)$$

$$= h \sum_{i < j} \sum_k \alpha_k^2 \rho_{ijk}^2 - g^2 \sum_{i < j} r_{ij}^{-3} \sum_k \alpha_k^2 \rho_{ijk}^2 \quad (9)$$

$$= h \sum_{i < j} r_{ij}^2 - g^2 \sum_{i < j} r_{ij}^{-3} r_{ij}^2 \quad (10)$$

$$= hg^2 - g^2 h. \quad (11)$$

The role of Eq. (2) in this development highlights a condition equivalent to radial invariance: that the value of any  $r_{ij}$  becomes scaled by  $t$  when moving from  $v_1^{(1)}, \dots, v_d^{(1)}$  to  $v_1^{(2)}, \dots, v_d^{(2)}$ .

**Shape complexity and clustering.** Increasing any  $r_{ij}$  always increases  $g$  while decreasing  $h$ . Notably, the most significant increases in  $g$  come from increasing the largest  $r_{ij}$ 's (since  $\partial g / \partial r_{ij} = g^{-1} r_{ij}$ ), while the most significant decreases in  $h$  come from increasing the smallest  $r_{ij}$ 's (since  $\partial h / \partial r_{ij} = -r_{ij}^{-2}$ ). Because increases in the  $r_{ij}$ 's are mediated by increases in the  $\alpha_k$ 's, the effect of increasing any specific  $\alpha_k$  on the  $r_{ij}$ 's of specific relative magnitudes is best understood by considering how the ratios  $g'_k/g$  and  $-h'_k/h$  relate to each other. Two cases must be considered, as follows.

- C1. If  $g'_k/g > -h'_k/h$  (i.e., increasing  $\alpha_k$  causes more of a relative increase in  $g$  than a relative decrease in  $h$ ), then larger  $r_{ij}$ 's are being increased more than smaller  $r_{ij}$ 's.
- C2. If  $g'_k/g < -h'_k/h$  (i.e., increasing  $\alpha_k$  causes more of a relative decrease in  $h$  than a relative increase in  $g$ ), then smaller  $r_{ij}$ 's are being increased more than larger  $r_{ij}$ 's.

In the context of data clustering, assume for a moment that larger  $r_{ij}$ 's are generally intercluster distances while smaller  $r_{ij}$ 's are generally intracluster distances. Cases C1 and C2 above are then in strong opposition to each other, as clearly case C1 could be good for clustering and case C2 bad for clustering. We might then expect to be well-off if we targeted case C1 for every  $k$ , but surely an assignment of values to  $\alpha_1, \dots, \alpha_d$  might satisfy case C1 for a specific  $k$  while satisfying case C2 for another. In this case it would seem better to pursue the intermediate goal of getting as close as possible to achieving  $g'_k/g = -h'_k/h$  for every  $k$ .

Real-world data, however, rarely comply with the dichotomy we momentarily assumed above. Instead, quite often larger distances are intracluster, and likewise smaller distances are intercluster. In any case, the centerpiece of the strategy we adopt henceforth is the same that would be appropriate had the dichotomy always held true, that is, seeking the equilibrium represented by  $g'_k/g = -h'_k/h$  for every  $k$ . On top of this, we essentially look for several

scaling-factor schemes approaching such conditions as closely as possible and select the one (or more than one) that upon closer inspection of the data leads to a reasonable partition into clusters.

**The optimization problem.** A consequence of our discussion of the radial-invariance property of SC is that all assignments of values to  $\alpha_1, \dots, \alpha_d$  on any straight line emanating from the origin into the positive  $d$ -dimensional real orthant are equivalent at providing scaling factors for distance-based clustering. That is, choosing any such assignment will lead any distance-based clustering algorithm to yield the same result. This follows from the fact that the  $r_{ij}$ 's for a given assignment on that line are scaled versions, by the same factor on all dimensions, of  $r_{ij}$ 's for any of the other assignments.

In what follows, all but one of such equivalent assignments are ignored. The one that is taken into account is that for which

$$\sum_k \alpha_k^2 = d. \quad (12)$$

That is, valid assignments of values to the  $\alpha_k$ 's must be on the  $d$ -dimensional sphere of radius  $\sqrt{d}$  centered at the origin. This choice of radius allows for  $\alpha_k = 1$  for every  $k$  to be a valid assignment. This, we recall from earlier in this section, is the assignment that scales the data along dimension  $k$  by the factor  $1/\sigma_k$ .

Seeking to approximate  $g'_k/g = -h'_k/h$  for every  $k$  given this equality constraint boils down to the problem of finding a local minimum or maximum of SC given the constraint. Because SC is inextricably based on the data to be clustered, it seems to have no characteristic that can be directly exploited to this end. We follow an indirect route and begin by considering the first-order necessary condition for local optimality in this case [15], which requires not only the equality constraint in Eq. (12) to be satisfied but also the gradient of the corresponding Lagrangian with respect to the  $\alpha_k$ 's to equal zero. The Lagrangian in this case is

$$L = \text{SC} + \lambda(\sum_k \alpha_k^2 - d), \quad (13)$$

where  $\lambda$  is the Lagrange multiplier corresponding to the single equality constraint. Its gradient's  $k$ th component is  $L'_k = g'_k h + g h'_k + 2\lambda \alpha_k$ . Writing this in more detail yields

$$L'_k = \alpha_k \left( g^{-1} h \sum_{i < j} \rho_{ijk}^2 - g \sum_{i < j} r_{ij}^{-3} \rho_{ijk}^2 + 2\lambda \right), \quad (14)$$

from which it follows that, in order to achieve  $L'_k = 0$  for every  $k$ , we must have

$$\sum_{i < j} r_{ij}^{-3} \frac{\rho_{ijk}^2}{\sum_{i < j} \rho_{ijk}^2} = \frac{g^{-1} h + 2\lambda (\sum_{i < j} \rho_{ijk}^2)^{-1}}{g} \quad (15)$$

for each of them.

Even though it would seem that the right-hand side of Eq. (15) may have a different value for each  $k$ , letting  $N = n_{\text{orig}}(n_{\text{orig}} - 1)$  we note that  $\sigma_k^2$  can be written as

$$\sigma_k^2 = N^{-1} \sum_{i < j} (X_{ik} - X_{jk})^2, \quad (16)$$

which leads to

$$\sum_{i < j} \rho_{ijk}^2 = N. \quad (17)$$

The right-hand side of Eq. (15) is therefore the same for every  $k$ , so its left-hand side, which is in fact the inner product of two vectors in  $\binom{n}{2}$ -dimensional real space, must also not depend on  $k$ . The  $ij$ th component of one of the two vectors involved in this inner product is  $N^{-1} \rho_{ijk}^2$ , so all  $d$  such vectors are coplanar, since by Eq. (17) they all lie on the  $\binom{n}{2}$ -dimensional plane  $\sum_{i < j} x_{ij} = 1$ . In order for the inner product to have the same value regardless of  $k$ , the vector of  $ij$ th component  $r_{ij}^{-3}$  must therefore be orthogonal to this plane. That is, we must have

$$\sum_{i < j} r_{ij}^{-3} N^{-1} (\rho_{ijk}^2 - \rho_{ij\ell}^2) = 0, \quad (18)$$

where  $k, \ell$  are any two of the  $d$  dimensions. In the formulation that follows we use  $k = 1, \ell = 2$ .

Determining the  $\alpha_k$ 's directly from Eq. (18) and the equality constraint is not possible, so we resort to the following nonlinear programming problem instead.

$$\text{minimize } \left( \sum_{i < j} r_{ij}^{-3} N^{-1} (\rho_{ij1}^2 - \rho_{ij2}^2) \right)^2 \quad (19)$$

$$\text{subject to } \sum_k \alpha_k^2 = d, \quad (20)$$

$$\alpha_k > 0. \quad \forall k \in \{1, \dots, d\} \quad (21)$$

Solving this problem will return  $\alpha_k$ 's that approximate Eq. (18) as well as possible. Even if a good approximation is returned, it must be kept in mind that only first-order necessary conditions are being taken into account. The second-order necessary and sufficient conditions, which involve the second derivatives of SC, are not. Further methodological steps must then be taken, as detailed in Section 3 along with the necessary tool set. Henceforth, we refer to the optimization problem given in Eqs. (19)–(21) simply as Problem P.

**Further remarks.** Another consequence of Eq. (17) is that

$$\sum_{i < j} r_{ij}^2 = N \sum_k \alpha_k^2, \quad (22)$$

which allows  $g$  to be rewritten as

$$g = \left( N \sum_k \alpha_k^2 \right)^{1/2}. \quad (23)$$

Table 1: Data sets used and their properties.

Data set, number of clusters	Number of samples ( $n_{\text{orig}}$ )	Number of unique samples ( $n$ )	Number of actual/original dimensions ( $d/d_{\text{orig}}$ )	Number of dimensions with missing values ( $d_{\text{miss}}$ )
Iris, 3	150	149	4/4	0
BCW, 2	699	465	9/9	1
BC-DR3, 4	62	62	3/496	392
BNA-DR3, 2	1372	1348	3/4	0
BCW-Diag-10, 2	569	569	10/30	0

### 3 Experimental setup

Solving Problem P to discover the  $\alpha_k$ 's is the centerpiece of our approach. Several candidate sets of these scaling factors can be obtained by solving the problem repeatedly in a sequence of random trials, each one first selecting an initial point for the minimization and then attempting to converge to a set of  $\alpha_k$ 's for which the problem's objective function is locally minimum. The resulting scaling-factor sets can then be pitched against one another, engaging the user's knowledge of the data set for the selection of a small set of candidates (perhaps even a single one) to carry on with.

Because clustering is an approach to data analysis that depends strongly on a domain expert's knowledge of and familiarity with the data set, uncertainties during the process of selecting appropriate scaling-factor sets from those turned up by solving Problem P are inevitable. To illustrate some strategies to deal with this, in Sections 4 and 5 we discuss our experience with analyzing five well-known benchmarks in light of SC. Dealing with these data sets has of course been greatly facilitated by the availability of the reference partition into clusters for each one. This will not be available in a real-world scenario, except perhaps in some fragmentary form, but in our discussion of the benchmarks we attempt to provide viewpoints that may be useful even then.

We continue this section with the presentation of the benchmarks we use, and of the tools, algorithms, and evaluation method we enlist.

**Data sets.** The five data sets we use are listed in Table 1, along with crucial information on them. We divide them into two groups, based on our experience in handling them, particularly on the difficulty in obtaining good partitions. The first group contains those for which it has proven possible to obtain partitions that approximate the corresponding reference partition well. The second group contains those for which approximating the reference partition, even if only reasonably, has proven harder.

The first group has two members, the Iris data set (downloaded from [16] and then corrected to exactly match the data in the original publication [17]) and BCW, the original version of the Wisconsin breast cancer data sets [18].



The second group comprises three data sets, viz.: BC-DR3, which comes from the version of Perou et al.’s breast cancer data set [19] compiled and made available by the proponents of scaling by the  $\sigma_k^{\text{pool}}$ ’s mentioned in Section 1; BNA-DR3, from a data set containing wavelet-transform versions and the entropy of banknote images for authentication [20]; and BCW-Diag-10, from the so-called diagnostic version of the Wisconsin breast cancer data sets [21].

The three data sets in the second group have fewer dimensions than originally available, which is indicated in Table 1 by the  $d < d_{\text{orig}}$  values on the fourth column. We reduced these data sets’ numbers of dimensions as an attempt to make clustering succeed better than it would otherwise. In two cases this is indicated by the “DR3” in the data sets’ names, which refers to dimensionality reduction by adopting the first three principal components output by principal component analysis (PCA) [22] on the data after centering (but not scaling) the samples. This was done in the R language, using function `prcomp` with options `center = T` and `scale = F`. The resulting BC-DR3 and BNA-DR3 retain 35.85% and 97.02% of the original variance, respectively.

The third case is that of BCW-Diag-10, which contains only the first 10 of the original 30 dimensions. Each sample in this data set is an image and each dimension is a statistic computed on that image. The 10 dimensions we use are mean values.

As per the second and third columns in the table, three of the data sets (Iris, BCW, and BNA-DR3) contain more samples ( $n_{\text{orig}}$ ) than unique samples ( $n$ ). The difference corresponds to duplicates, which were discarded so that SC, and consequently Problem P, could be defined properly. The table’s fifth column is also worthy of attention, since it gives for each data set the number of dimensions ( $d_{\text{miss}}$ ) for which missing values are to be found. Such values were synthesized in the Wolfram Mathematica 13.0 system, using function `SynthesizeMissingValues` with default settings. This caused no further duplicates to appear and, in the case of BC-DR3, was of course done before PCA.

**Computational tools and algorithms.** For each of the data sets in Table 1, first we ran 1 000 trials, each one aiming to obtain a scaling-factor candidate set by solving Problem P. We did the required optimization in the Wolfram Mathematica 13.0 system, using function `FindMinimum`, mostly with default settings, to find a local minimum of the problem’s objective function for each trial. Our only choices of a non-default setting for `FindMinimum` were the following: for each trial we specified an initial point in  $[0.5, 1.5]^d$ , selected uniformly at random by an application of function `RandomReal` to each dimension; we allowed for a larger number of iterations with the `MaxIterations -> 5000` option; and we precluded any symbolic manipulation with `Gradient -> "FiniteDifference"` (because Problem P is strongly data-dependent, allowing Mathematica to perform the symbolic manipulations that come so naturally to it can quickly lead to memory overflow).

On occasion we have noticed that coding the constraint in Eq. (21) as is can lead to division-by-zero errors. We thus avoided this by expressing the constraint as  $\alpha_k \geq 10^{-5}$  instead of  $\alpha_k > 0$ . Still regarding errors during minimization, `FindMinimum` can also fail by not attaining convergence within the specified maximum number of iterations. This error can take more than one form, but in general we have observed it in no more than 0.2% of the trials for each data set. When a failure of this type does occur a solution is still output, but in our experiments such outputs were discarded when compiling results.

One crucial step in this study is of course partitioning the data into clusters after they have been appropriately scaled. We performed this step in the R language, using in all cases the k-means method as implemented in function `kmeans`. Because k-means has certain randomized components, we first set a fixed seed, via `set.seed(1234)`, to facilitate consistency checks. Function `kmeans` receives as input the scaled version of the  $n_{\text{orig}} \times d$  data matrix  $X$  and also the desired number of clusters (the same as in the data set’s reference partition). For the results we report in Section 4, scaling happened according to one of four possibilities: either each  $X_{ik}$  remained unchanged (no scaling), or it became one of  $(1/\sigma_k)X_{ik}$ ,  $(1/\sigma_k^{\text{pool}})X_{ik}$ , or  $(\alpha_k/\sigma_k)X_{ik}$ . The latter is scaling as indicated by some random trial with Problem P.

**Partition evaluation.** To evaluate the partition resulting from clustering we use the variant of the well-known Adjusted Rand Index (ARI) [23] that seems most appropriate in our present context, which is that every possible resulting partition of a data set by the clustering algorithm in use must have a fixed number of clusters (“fnc,” used in notations henceforth) [24]. That this is clearly the case follows from our use of k-means described above. The ARI variant is

$$\text{ARI}_{\text{fnc}} = \frac{\text{RI} - \text{E}_{\text{fnc}}[\text{RI}]}{1 - \text{E}_{\text{fnc}}[\text{RI}]}, \quad (24)$$

where RI is the original Rand Index and  $\text{E}_{\text{fnc}}[\text{RI}]$  is its expected value given the fixed number of clusters condition.

Letting  $C$  denote the number of clusters that any obtained partition will have, the formulas for RI and  $\text{E}_{\text{fnc}}[\text{RI}]$  are

$$\text{RI} = \binom{n_{\text{orig}}}{2}^{-1} (\text{TS} + \text{TD}) \quad (25)$$

and

$$\text{E}_{\text{fnc}}[\text{RI}] = UV + (1 - U)(1 - V), \quad (26)$$

with

$$U = \left\{ \begin{matrix} n_{\text{orig}} \\ C \end{matrix} \right\}^{-1} \left\{ \begin{matrix} n_{\text{orig}} - 1 \\ C \end{matrix} \right\} \quad (27)$$

and

$$V = \binom{n_{\text{orig}}}{2}^{-1} (\text{TS} + \text{FD}). \quad (28)$$

Table 2: Performance of k-means, according to  $\text{ARI}_{\text{fnc}}$ , on various scaled versions of the data sets in Table 1.

Data set	$\text{ARI}_{\text{fnc}}$			
	No scaling	Scaling by $1/\sigma_k$	Scaling by $1/\sigma_k^{\text{pool}}$	Scaling by $\alpha_k/\sigma_k$
Iris	0.728	0.621	0.886	0.571–0.904
BCW	0.840	0.825	0.825	0.189–0.877
BC-DR3	0.492	0.518	0.518	(−0.021)–0.535
BNA-DR3	0.050	0.023	0.023	(−0.000)–0.659
BCW-Diag-10	0.456	0.673	0.673	0.633–0.655

In Eqs. (25) and (28), TS (for “true similar”) counts the number of sample pairs that are in the same cluster according to the obtained partition and in the same cluster according to the reference partition; TD (“true dissimilar”) counts pairs that are split between different clusters according to both the obtained partition and the reference partition; and FD (“false dissimilar”) counts those that are split between different clusters according to the obtained partition but are in the same cluster according to the reference partition. Curly brackets are used in Eq. (27) to denote Stirling numbers of the second kind.

$\text{ARI}_{\text{fnc}}$  equals at most 1, which happens for  $\text{TS} + \text{TD} = \binom{n_{\text{orig}}}{2}$  (i.e., when the obtained partition and the reference partition are identical).

## 4 Results

All our results are in reference to the data sets listed in Table 1 and are summarized in Table 2. In this table, the value of  $\text{ARI}_{\text{fnc}}$  resulting from the use of k-means is given for each of several scaled versions of the  $n_{\text{orig}} \times d$  data matrix  $X$  that corresponds to each data set. There are four schemes in each case: the no-scaling scheme, in which each  $X_{ik}$  is used directly as it appears in the data matrix; the scheme that makes use of the standard deviation in each dimension, in which  $X_{ik}$  is scaled by  $1/\sigma_k$ ; the scheme that uses pooled standard deviations instead, in which  $X_{ik}$  is scaled by  $1/\sigma_k^{\text{pool}}$ ; and the scheme that uses scaling factors obtained by solving Problem P, in which  $X_{ik}$  is scaled by  $\alpha_k/\sigma_k$  for the resulting  $\alpha_k$ .

$\text{ARI}_{\text{fnc}}$  values for the latter type of scaling are presented in Table 2 as intervals, indicating in each case the lowest and the highest value observed in the 1 000 random trials with Problem P (slightly fewer trials if optimization errors happened). For BC-DR3 and BNA-DR3, the intervals begin at slightly negative values of  $\text{ARI}_{\text{fnc}}$  (indicating that  $\text{RI} < \text{E}_{\text{fnc}}[\text{RI}]$ ).

The intervals on the rightmost column of Table 2 are supplemented by the panels in Figure 1, where each row of panels (rows A through E) corresponds to one of the data sets. Such panels allow viewing the various  $\text{ARI}_{\text{fnc}}$  values inside those intervals from different perspectives. The left panel on each row is a plot of SC against  $\alpha_1$  for all trials on the corresponding data set. The choice

of  $\alpha_1$  is completely arbitrary and meant only to offer a glimpse into how SC depends on the  $\alpha_k$ 's turned up by solving Problem P. Points are color-coded to indicate how their  $\text{ARI}_{\text{fnc}}$  values relate to one another. The right panel on each row allows viewing such values as a histogram.

## 5 Discussion

Table 2 confirms, for the selection of data sets we are considering, what by and large has been known for a long while. That is, that scaling by  $1/\sigma_k$  can sometimes be worse than simply attempting to partition the data in  $X$  into clusters without any scaling. In the table, this is the case mainly of the Iris data set. Table 2 also confirms what has been known since the recent introduction of scaling by  $1/\sigma_k^{\text{pool}}$ , which is that proceeding in this way, once again in the case of Iris, leads to superior performance. The table goes farther than this, however, since it also makes clear that the fallback role of  $\sigma_k$  as a surrogate for  $\sigma_k^{\text{pool}}$  in the approach of [5] may be taken more frequently than initially realized. This is shown in the table for all but the Iris data set.

But the most relevant contribution of the results in Table 2 is the realization that in almost all cases the best performing set of  $\alpha_k$ 's for each data set performs strictly better than the other three alternatives. The only exception is the BCW-Diag-10 data set, although in this case every one of the sets of  $\alpha_k$ 's can be said to lie, so to speak, in the same ballpark as  $1/\sigma_k$  (or  $1/\sigma_k^{\text{pool}}$ ). In fact, the plots in Figure 1(E) strongly suggest that scaling the data for BCW-Diag-10 by the outcome of virtually any of the random trials with Problem P would be equally acceptable. This would be so even if a reference partition (and hence  $\text{ARI}_{\text{fnc}}$  values) had not been available, because comparing the obtained partitions with one another would already suffice.

Of course, the latter is based almost entirely on the highly concentrated character of the  $\text{ARI}_{\text{fnc}}$  histogram in Figure 1(E), which to a degree is also true of Figures 1(B) and 1(C), which refer to the BCW and BC-DR3 data sets, respectively. For each of these two data sets, comparing the partitions resulting from the random trials with Problem P with one another, and adopting any of those that by the  $\text{ARI}_{\text{fnc}}$  histogram seem not only to be one and the same but also to recur very frequently during the trials, would lead to equally acceptable scaling decisions.

This leaves us with the Iris and BNA-DR3 data sets. In these two cases, choosing the set of  $\alpha_k$ 's to use out of those produced by the random trials with Problem P by simply comparing the obtained partitions and looking for a consensus with strong support would lead to disastrous results. This is clear from the  $\text{ARI}_{\text{fnc}}$  histograms in Figures 1(A) and 1(D), which peak significantly to the left of the best values attained in the trials. Beyond comparing obtained partitions, one must therefore also use one's knowledge of the domain in question and look at what they are doing to the data. The guiding principle to be used is essentially in the spirit of our discussion in Section 2: in the end, the candidate set of  $\alpha_k$ 's to be chosen must lead to a partition that makes sense, either visually

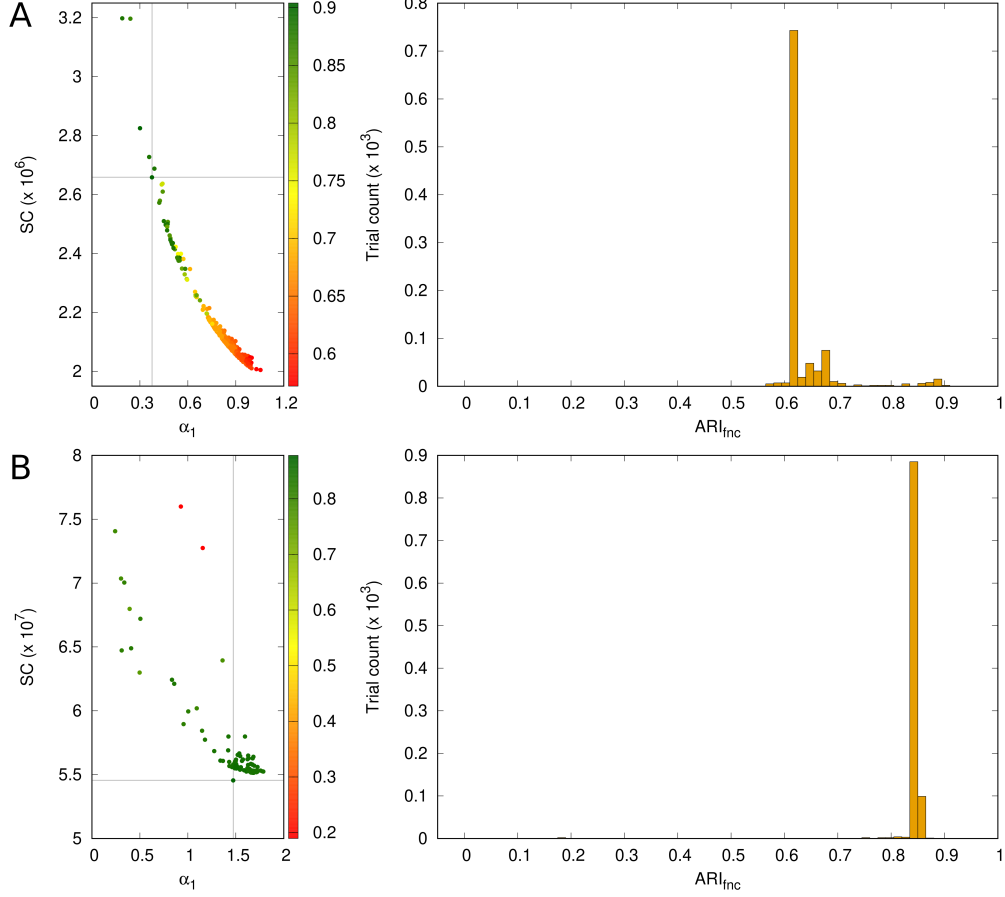


Figure 1: Results of the random trials with Problem P on Iris (A), BCW (B), BC-DR3 (C), BNA-DR3 (D), and BCW-Diag-10 (E), expanding on the summary given on the rightmost column of Table 2. Each point on each left panel corresponds to a trial and is color-coded according to the accompanying palette to reflect the value of  $ARI_{fnc}$  it leads to by way of clustering with k-means. The point leading to the highest  $ARI_{fnc}$  value is marked by the crosshair in the panel. Each right panel provides a view of how  $ARI_{fnc}$  is distributed over all pertaining trials.

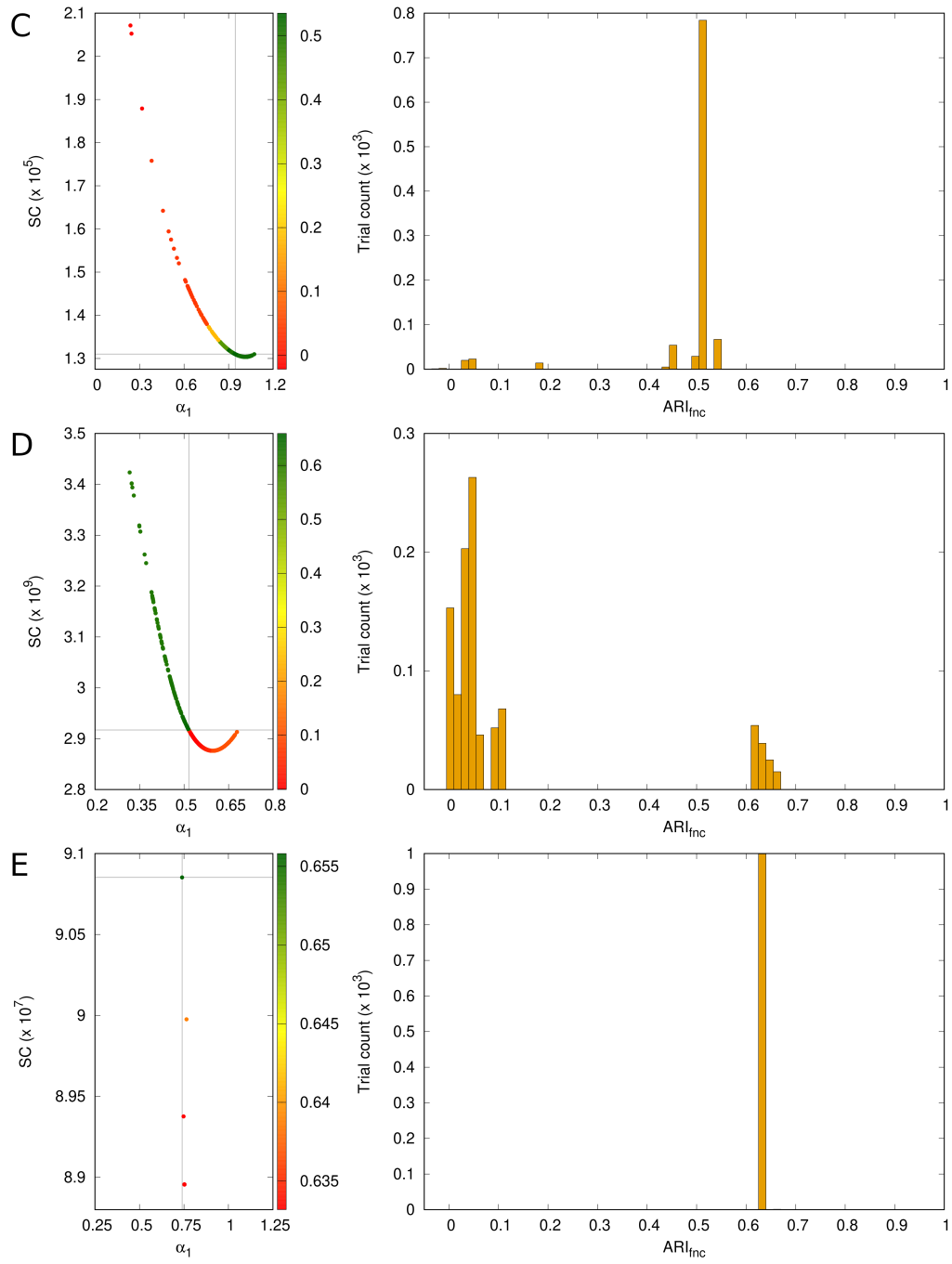


Figure 1: Continued.

Table 3: Scaling factors used in Figures 2 (Iris) and 3 (BNA-DR3). The  $\alpha_k$ ’s are the ones leading to the highest values of  $\text{ARI}_{\text{fnc}}$  in the intervals on the rightmost column of Table 2.

$k$	Iris		BNA-DR3	
	$1/\sigma_k$	$\alpha_k/\sigma_k$	$1/\sigma_k$	$\alpha_k/\sigma_k$
1	1.207	0.453	0.141	0.073
2	2.294	1.291	0.327	0.373
3	0.566	0.859	0.477	0.571
4	1.311	1.459		

or by inspection of the “midrange” distances between samples, those that can be more easily mistaken for intracluster when they are intercluster or conversely.

We proceed with the aid of Table 3, which lists each  $1/\sigma_k$  and each  $\alpha_k/\sigma_k$  (this one for the highest  $\text{ARI}_{\text{fnc}}$  listed in Table 2) for Iris and BNA-DR3. Note, for the Iris data set, that  $k = 1$  and  $k = 3$  are the dimensions for which switching from scaling by  $1/\sigma_k$  to scaling by  $\alpha_k/\sigma_k$  provides the greatest scaling-factor reduction and amplification (given, in fact, by the value of  $\alpha_k$ ), respectively. For the BNA-DR3 data set, dimension  $k = 1$  has its weight on distances strongly reduced in moving from the former scaling scheme to the latter, while for both  $k = 2$  and  $k = 3$  the scaling factor is amplified by about the same proportion.

For the Iris data set, in Figure 2 we give six panels. These are arranged in three columns, the leftmost one dedicated to the data set’s reference partition, each of the other two to a different scaling scheme (scaling by  $1/\sigma_k$  and scaling by  $\alpha_k/\sigma_k$ , with factors as in Table 3). The top panel in each column contains a scatterplot of the samples, each color-coded for the data set’s three classes, as represented by dimensions  $k = 1$  and  $k = 3$  (cf. the discussion above in reference to Table 3). The bottom panel is a histogram of the  $r_{ij}$ ’s, the distances between samples in  $d$ -dimensional real space. It is important to emphasize that, in regard to the leftmost column, and unlike what happens with the other two, the scatterplot in it is color-coded to reflect the reference partition, not the obtained partition that results from the no-scaling scheme.

As we examine the scatterplots in the figure we see that scaling by  $1/\sigma_k$  stretches dimension  $k = 1$  excessively just as dimension  $k = 3$  is excessively shrunk, resulting in more confusion between the two clusters that are not linearly separable. We also see why scaling by  $\alpha_k/\sigma_k$  as in Table 3 is a better choice: the previous stretching of dimension  $k = 1$  and the shrinking of dimension  $k = 3$  are both undone, though to different degrees, which allows some of the previously added confusion to be reverted. Examining the distance histograms reveals that scaling by  $1/\sigma_k$  causes distances to become more concentrated, lengthening some of the smallest ones and shortening some of the largest. So another way to view the further confusion added by this scaling scheme is to recognize that it affects the already potentially problematic midrange distances. Scaling by  $\alpha_k/\sigma_k$  restores the overall appearance of the no-scaling histogram (the one in the leftmost column), but seemingly with sharper focus around those distances.

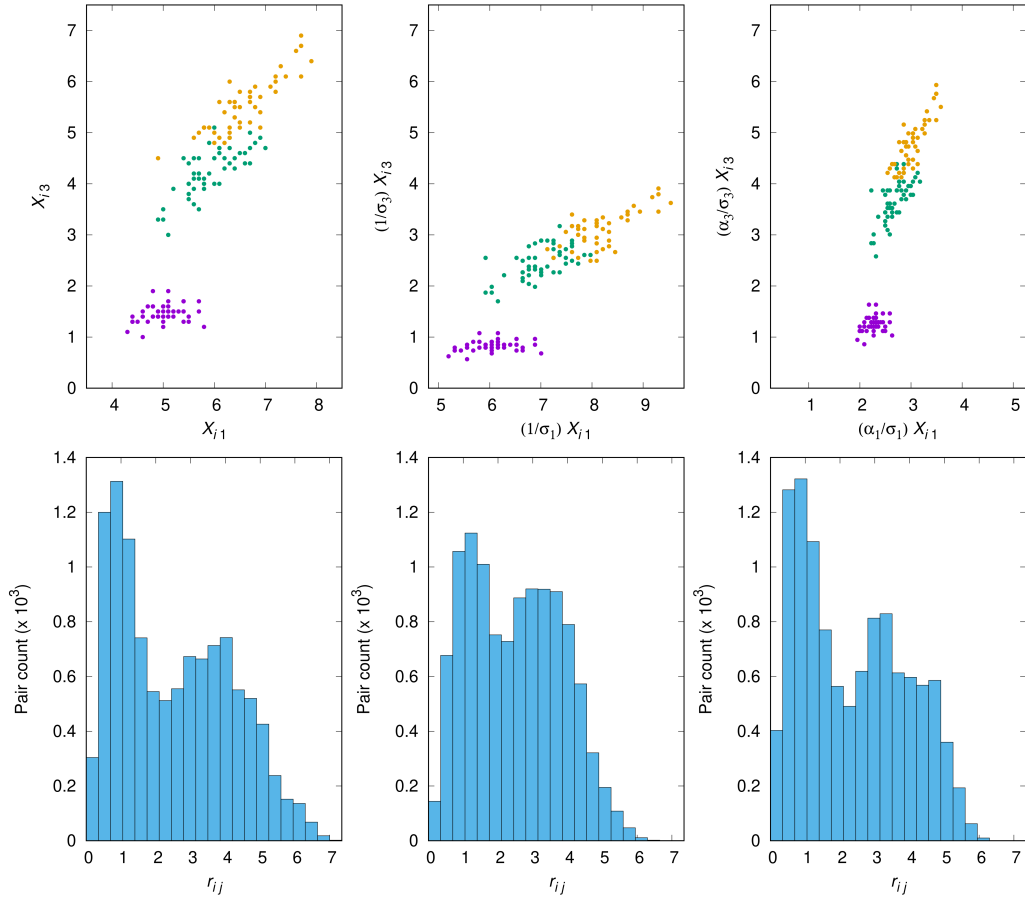


Figure 2: Reference partition for the Iris data set (leftmost column of panels) and the effects of two scaling schemes: scaling by  $1/\sigma_k$  (middle column) and scaling by  $\alpha_k/\sigma_k$  (rightmost column), with factors as in Table 3. Effects can be seen both with respect to the shape of the data set (top row of panels, all plots drawn to the same scale) and to the distribution of distances between samples (the  $r_{ij}$ 's; bottom row, all plots drawn to the same scale).



This is important because, as we know from Table 2, scaling the Iris data set by the  $\alpha_k/\sigma_k$  factors of Table 3 improves not only on the use of the  $1/\sigma_k$  factors but also on the no-scaling scheme, on which k-means already performs more than reasonably well.

Figure 3 has the same six panels as Figure 2, and also identically arranged, but now referring to the BNA-DR3 data set. This data set provides a much more striking contrast between the two scaling schemes given in Table 3 than Iris, as per Table 2 the ratio of the  $\text{ARI}_{\text{fnc}}$  value that scaling by  $\alpha_k/\sigma_k$  yields to that of scaling by  $1/\sigma_k$  is about 28.65.

The most direct pictorial evidence we have of this comes from comparing the middle and rightmost scatterplots of Figure 3 with each other, having the leftmost one as the reference partition. Because the ratio of  $\alpha_k/\sigma_k$  to  $1/\sigma_k$  (i.e., the value of  $\alpha_k$ ) is slightly higher than only 1.1 for both  $k = 2$  and  $k = 3$  (once again, cf. our earlier comment on this), what really accounts for the very significant difference between the two scaling schemes has to do with dimension  $k = 1$ , for which a ratio of about 0.517 ensues. Visually inspecting the two obtained partitions vis-à-vis the reference partition provides immediate confirmation of how crucial this shrinking of dimension  $k = 1$  is. As with the Iris data set, inspecting the histograms in the figure provides insight similar to the one we gleaned in that case. Even though the middle and rightmost histograms, corresponding respectively to scaling by  $1/\sigma_k$  and  $\alpha_k/\sigma_k$ , may seem similar to each other particularly when viewed in comparison to the no-scaling histogram (the leftmost one), closer inspection tells a different story. That is, moving from scaling by  $1/\sigma_k$  to scaling by  $\alpha_k/\sigma_k$  seems to restore some of the no-scaling histogram’s slow descent from its peak through the midrange distances. This comes about by virtue of both a lower peak and the appearance of some residual pair count beyond the  $r_{ij} = 5$  bar when the additional  $\alpha_k$  factor is put to use. This is curious, especially as we note from Table 2 that no scaling and scaling by  $1/\sigma_k$  both lead k-means to essentially the same poor performance. This seems to be suggesting that, in the no-scaling scheme, such poor performance is to be attributed essentially to the excessive spread of distances.

## 6 Concluding remarks

In this paper we have revisited the problem of scaling a data set’s dimensions to facilitate clustering by those methods that, like k-means, make explicit use of distances between samples. For each dimension  $k$ , we have framed our study as the determination of a scale factor  $\alpha_k > 0$  to be applied on top of the customary division by  $\sigma_k$ , the standard deviation of the data in that dimension. That is, we have targeted a scaling factor of the form  $\alpha_k/\sigma_k$ . Our guiding principle has been to focus on the effects of scaling the data on the multidimensional shapes that ensue: essentially, we have equated any facilitation of the clustering task with mistaking intercluster distances for intracluster distances (or conversely) as seldom as possible. Because we normally think of the former type of distances as

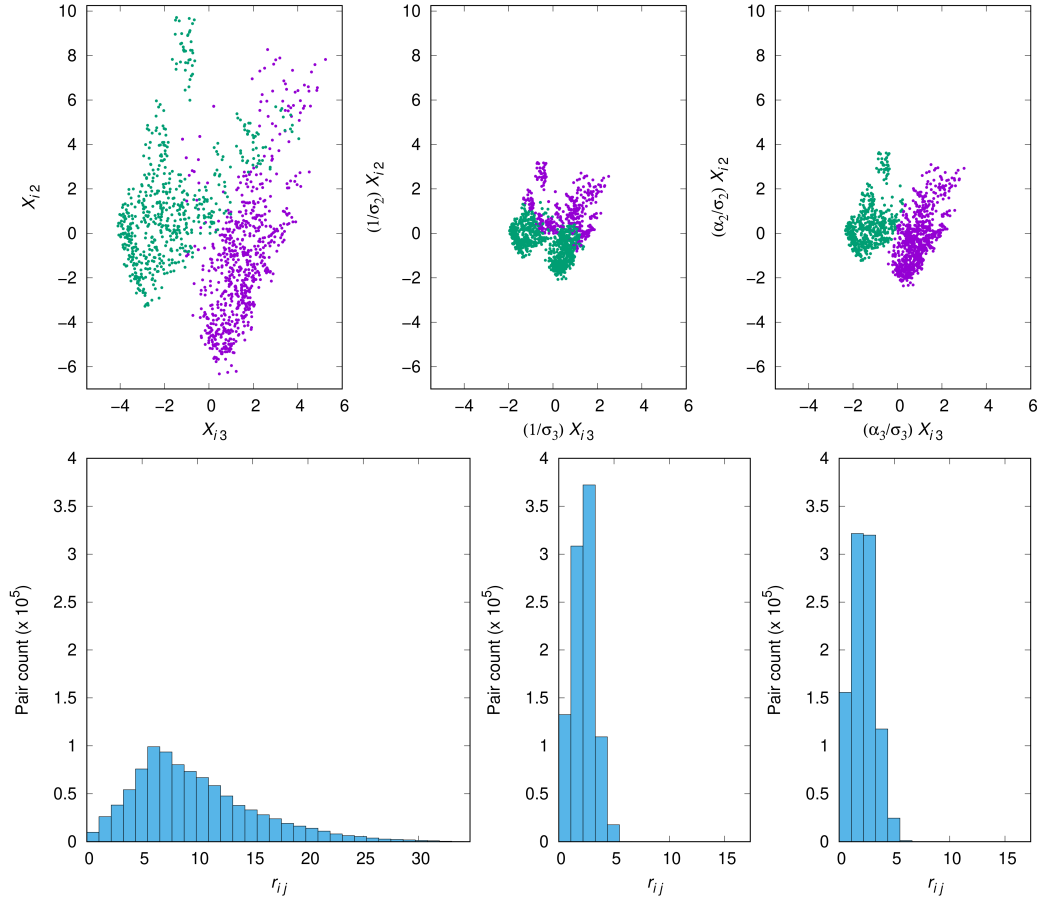


Figure 3: As in Figure 2, now for the BNA-DR3 data set.

being large, and the latter as being small, we have aimed our efforts at midrange distances.

To make such notions precise, we enlisted the shape complexity of the scaled data, given by SC, which depends heavily on the data matrix  $X$  (as a constant) and on the various  $\alpha_k$ 's (as variables). The function SC embodies a lot of the tension between large and small distances between samples and, as such, allows midrange distances to be characterized as being the equilibrium between extremes that occurs at those  $\alpha_k$ 's for which the gradient of SC is zero. We have viewed such scaling-factor sets as candidates, each one obtained by solving Problem P, given in Eqs. (19)–(21), from a randomly chosen initial point.

All our results refer to data sets that are essentially manageable when considering both their numbers of samples and numbers of dimensions. The performance of k-means clustering on them, as measured by  $\text{ARI}_{\text{fnc}}$ , ranges from very poor to well above average, so calling them “manageable” refers not at all to how amenable to clustering by k-means they are, but rather to the possibility of solving Problem P for them multiple times without too much computational effort.

Our results can be summarized very simply: for all data sets we tackled, generating scaling-factor candidate sets via Problem P has yielded at least one set for which scaling by  $\alpha_k/\sigma_k$  (as opposed to  $1/\sigma_k$ ) leads to strictly better performance (with one single exception, where “strictly better” becomes “comparable”). The overall method cannot be used as a blind procedure, though, since in at least two cases we came across the need for carefully considered visual inspections of the scaled data, perhaps even of their distance histograms.

In spite of the radial invariance of SC, which we used to constrain the  $\alpha_k$ 's when formulating Problem P, the number of possibilities outside the reach of Problem P is limitless. Suppose, for example, that we use the following alternative formulation of the nonlinear programming problem.

$$\text{maximize SC} \tag{29}$$

$$\text{subject to } \alpha_k \geq 10^{-5}, \quad \forall k \in \{1, \dots, d\} \tag{30}$$

In significant ways this is still in the spirit of Problem P, even though it limits the notion of a gradient-zero point to those that correspond to local maxima of SC. We mention this particular formulation because solving it for the Iris data set, as explained in Section 3 for Problem P (now with **FindMaximum** substituting for **FindMinimum** and selecting the initial points from  $[10^{-5}, 1]^d$ ), yielded  $\text{ARI}_{\text{fnc}} = 0.922$  in the best case, with  $\alpha_1 = \alpha_2 = 10^{-5}$ ,  $\alpha_3 = 5.09372 \times 10^{17}$ , and  $\alpha_4 = 2.48504 \times 10^{17}$ . This is an interesting outcome, and not only because it surpasses the best result reported in Table 2 ( $\text{ARI}_{\text{fnc}} = 0.904$ ). What these  $\alpha_k$ 's are saying is: reduce the importance of dimensions  $k = 1$  and  $k = 2$  as far as allowed by the constraint in Eq. (30) while dimensions  $k = 3$  and  $k = 4$  are very strongly amplified. This is to a degree already what Table 3 is suggesting, though only in relation to scaling by  $1/\sigma_k$  and moreover much more timidly.

Alternative formulations like this, and the surprising results they may lead to, serve to illustrate the rich store of possibilities for shape complexity-based

cluster analysis. Additional investigations to further explore SC and its role in helping determine appropriate scaling factors for any given data set could well be worth the effort. A crucial ingredient will be the use of techniques to not only reduce the number of dimensions in the data, but also the number of samples (e.g., as discussed in [25]), aiming to make possible the solution of problems like Problem P. In this regard, we note that, already for the precursor of the BC-DR3 data set, with  $n_{\text{orig}} = 62$  and  $d_{\text{orig}} = 496$ , solving one trial with Problem P is expected to take a few hundred hours.

## Acknowledgments

The authors acknowledge partial support from Conselho Nacional de Desenvolvimento Científico e Tecnológico (CNPq), Coordenação de Aperfeiçoamento de Pessoal de Nível Superior (CAPES), and a BBP grant from Fundação Carlos Chagas Filho de Amparo à Pesquisa do Estado do Rio de Janeiro (FAPERJ).

## References

- [1] R. A. van den Berg, H. C. J. Hoefsloot, J. A. Westerhuis, A. K. Smilde, and M. J. van der Werf. Centering, scaling, and transformations: improving the biological information content of metabolomics data. *BMC Genomics*, 7:142, 2006.
- [2] C. Edelbrock. Mixture model tests of hierarchical clustering algorithms: the problem of classifying everybody. *Multivariate Behavioral Research*, 14:867–884, 1979.
- [3] G. W. Milligan and M. C. Cooper. A study of standardization of variables in cluster analysis. *Journal of Classification*, 5:181–204, 1988.
- [4] D. Steinley. Standardizing variables in k-means clustering. In D. Banks, F. R. McMorris, P. Arabie, and W. Gaul, editors, *Classification, Clustering, and Data Mining Applications*, pages 53–60. Springer-Verlag, Berlin, Germany, 2004.
- [5] J. Raymaekers and R. H. Zamar. Pooled variable scaling for cluster analysis. *Bioinformatics*, 36:3849–3855, 2020.
- [6] J. B. Kruskal. Linear transformations of multivariate data to reveal clustering. In R. N. Shepard, A. K. Romney, and S. B. Nerlove, editors, *Multidimensional Scaling: Theory and Applications in the Behavioral Sciences*, volume 1. Theory, pages 181–191. Seminar Press, New York, NY, 1972.
- [7] W. S. DeSarbo, J. D. Carroll, and L. A. Clark. Synthesized clustering: a method for amalgamating alternative clustering bases with differential weighting of variables. *Psychometrika*, 49:57–78, 1984.

- [8] G. De Soete, W. S. DeSarbo, and J. D. Carroll. Optimal variable weighting for hierarchical clustering: an alternating least-squares algorithm. *Journal of Classification*, 2:173–192, 1985.
- [9] J. Hohenegger. Weighted standardization: a general data transformation method preceding classification procedures. *Biometrical Journal*, 28:295–303, 1986.
- [10] J. Rossignac. Shape complexity. *The Visual Computer*, 21:985–996, 2005.
- [11] F. Mercati. *Shape Dynamics: Relativity and Relationalism*. Oxford University Press, New York, NY, 2018.
- [12] J. Barbour. *The Janus Point: A New Theory of Time*. Basic Books, New York, NY, 2020.
- [13] P. Fränti and S. Sieranoja. K-means properties on six clustering benchmark datasets. *Applied Intelligence*, 48:4743–4759, 2018.
- [14] A. K. Jain. Data clustering: 50 years beyond k-means. *Pattern Recognition Letters*, 31:651–666, 2010.
- [15] D. G. Luenberger. *Introduction to Linear and Nonlinear Programming*. Addison-Wesley, Reading, MA, 1973.
- [16] Iris data set. <https://archive.ics.uci.edu/ml/datasets/Iris>. Accessed: 2022-03-19.
- [17] R. A. Fisher. The use of multiple measurements in taxonomic problems. *Annals of Eugenics*, 7:179–188, 1936.
- [18] Breast cancer Wisconsin (original) data set. [https://archive.ics.uci.edu/ml/datasets/breast+cancer+wisconsin+\(original\)](https://archive.ics.uci.edu/ml/datasets/breast+cancer+wisconsin+(original)). Accessed: 2022-03-19.
- [19] C. M. Perou, T. Sørli, M. B. Eisen, M. van de Rijn, S. S. Jeffrey, C. A. Rees, J. R. Pollack, D. T. Ross, H. Johnsen, L. A. Akslen, Ø. Fluge, A. Pergamenschikov, C. Williams, S. X. Zhu, P. E. Lønning, A.-L. Børresen-Dale, P. O. Brown, and D. Botstein. Molecular portraits of human breast tumours. *Nature*, 406:747–752, 2000.
- [20] Banknote authentication data set. <https://archive.ics.uci.edu/ml/datasets/banknote+authentication>. Accessed: 2022-03-19.
- [21] Breast cancer Wisconsin (diagnostic) data set. [https://archive.ics.uci.edu/ml/datasets/breast+cancer+wisconsin+\(diagnostic\)](https://archive.ics.uci.edu/ml/datasets/breast+cancer+wisconsin+(diagnostic)). Accessed: 2022-03-19.
- [22] I. T. Jolliffe and J. Cadima. Principal component analysis: a review and recent developments. *Philosophical Transactions of the Royal Society A*, 374:20150202, 2016.

- [23] L. Hubert and P. Arabie. Comparing partitions. *Journal of Classification*, 2:193–218, 1985.
- [24] A. J. Gates and Y.-Y. Ahn. The impact of random models on clustering similarity. *Journal of Machine Learning Research*, 18:1–28, 2017.
- [25] S. Eschrich, J. Ke, L. O. Hall, and D. B. Goldgof. Fast accurate fuzzy clustering through data reduction. *IEEE Transactions on Fuzzy Systems*, 11:262–270, 2003.